

Efficient Knowledge Infusion via KG-LLM Alignment

Anonymous ACL submission

Abstract

To tackle the problem of domain-specific knowledge scarcity within large language models (LLMs), knowledge graph-retrieval-augmented method has been proven to be an effective and efficient technique for knowledge infusion. However, existing approaches face two primary challenges: knowledge mismatch between public available knowledge graphs and the specific domain of the task at hand, and poor information compliance of LLM with knowledge graphs. In this paper, we leverage a small set of labeled samples and a large-scale corpus to efficiently construct domain-specific knowledge graphs by LLM, addressing the issue of knowledge mismatch. Additionally, we propose a three-stage KG-LLM alignment strategy to enhance the LLM’s capability to utilize information from knowledge graphs. We conduct experiments with a limited-sample setting on two biomedical question-answering datasets, and the results demonstrate that our approach outperforms existing baselines.

1 Introduction

Recent advancements in large language models (LLMs), such as ChatGPT, have demonstrated impressive capabilities in general-purpose content creation (OpenAI, 2022; Touvron et al., 2023). Nevertheless, their proficiency in domain-specific applications, particularly in the medical field, is notably constrained by insufficient knowledge (Bao et al., 2023; Zhang et al., 2023; Han et al., 2023b). To enhance the domain-specific performance of LLMs, the primary strategies for knowledge infusion include two main approaches: continual pre-training on domain-specific corpora and retrieval-augmented method, which involves integrating external information into the models.

Compared to continual pre-training, the retrieval-augmented approach is gaining popularity in knowledge-intensive scenarios due to its cost efficiency and enhanced traceability (Lewis et al.,

2020; Lan et al., 2023). Some retrieval-augmented method involve integrating LLMs with resources directly such as corpora, news articles and tables through supervised fine-tuning (Borgeaud et al., 2022; Hu et al., 2023). However, the knowledge required by the model may be scattered among vast amounts of data, and directly retrieving from raw data instances will introduce noise inevitably, preventing the model from effectively utilizing the information. To mitigate this issue, leveraging structured knowledge, especially knowledge graphs (KGs), is an effective method (Moiseev et al., 2022; Ranade and Joshi, 2023; Wang et al., 2023).

However, the existing KG-retrieval-augmented methods still encounter two principal challenges. The first challenge pertains to knowledge mismatch. While many existing strategies utilize public KGs for knowledge infusion, the knowledge demanded by domain-specific tasks is frequently of a highly specialized nature, leading to a substantial likelihood that the KG might not cover all the requisite information, or might even present gaps. The second challenge involves poor information compliance. The structured format of triples in KGs diverges from the free-flowing format of natural language (Li et al., 2021; Ke et al., 2021) and the target text often includes additional information that is not found in the triples. This disparity can lead to confusion within LLMs, which could result in outputs from the trained model that do not align with the information incorporated from the KG, particularly in scenarios with a scarcity of supervised examples.

In this work, we construct a domain-specific corpus-based knowledge graph efficiently by LLMs and develop a knowledge infusion approach to enhance the ability of LLMs to utilize graph information, enabling them to generate comprehensive, logical, and low-hallucination responses. Firstly, we train a knowledge extraction model based on LLM using a small amount of labeled data. Then, we ob-

tain a domain knowledge graph that resolves knowledge mismatch by performing extraction on unsupervised domain-specific corpora and reducing errors in the results through simple post-processing. Subsequently, we propose a novel three-phase KG-LLM alignment framework to optimize the exploitation of KG content by LLMs. The framework consists of the following stages:

- In the initial pre-learning phase, we synthesize substantial triples-to-text generation task examples derived from the previously mentioned extraction outcomes. We then train a Low-Rank Adapter(LoRA) (Hu et al., 2021), designated as K-LoRA, to assimilate the process of KG infusion and acquire proficiency in the domain-specific linguistic modality.
- The subsequent phase involves supervised fine-tuning. For each question-answer pair in the training set, we retrieve knowledge graph based on the question, concatenate the resultant subgraph into the input and proceed to train an additional LoRA. This process is designed to refine the model’s output, tailoring it to the specific demands of the given task.
- The final phase is the reinforcement learning from knowledge graph feedback (RLKGF). In this phase, we extract knowledge triples from the generated responses and compare them with the KG to provide evaluative feedback on the knowledge correctness. This feedback serves as a basis for further fine-tuning the model to achieve more comprehensive, less hallucinatory, and more logical content.

To simulate a realistic context where specialized annotations are scarce, we conduct experiments on limited-sample datasets constructed based on two public biomedical question answering datasets, BioASQ (Nentidis et al., 2022) and CMedQA (Cui and Han, 2020). In summary, our main contributions are as follows:

- 1) We propose a modular knowledge infusion framework. Building upon the efficiently constructed KG, our approach aligns LLMs with the KG through lightweight parameter adjustment, addressing issues of knowledge mismatch and poor information compliance. Experimental results demonstrate that our method significantly outperforms the baselines.

- 2) We introduce two innovative strategies, namely "pre-learning" and "RLKGF", aiming at forging a stronger link between KGs and LLMs. In pre-learning, we demonstrate that triples-to-text task can serve as a simple and effective knowledge infusion strategy. In RLKGF, we illustrate that KGs can function as automated evaluators for the knowledge correctness of generated responses.

2 Related Works

Retrieval-augmented LLMs. Retrieval-augmented generation methods (Izacard and Grave, 2021; Lewis et al., 2020; Min et al., 2023; Borgeaud et al., 2022) retrieve relevant information from an external database for the query and enable the LLM to generate results using this information. ChainRAG (Xu et al., 2023) focuses on addressing the problem of incorrect knowledge retrieved by information retrieval systems, which can mislead the LLM or disrupt its reasoning chain through their interaction. While these methods enhance factuality, they also introduce new hallucinations. To address this challenge, WebBrain (Qian et al., 2023) incorporates both specific information and general knowledge, which are intertwined with text snippets and used as references to complete the task.

LLM-augmented KG Construction. AutoKG (Yu et al., 2021) proposes a framework for constructing a KG from unstructured documents using information extraction (IE) and internal semantic alignment. Since the graphs constructed by IE typically suffer from edge sparsity and node redundancy, Wu et al. (2023) have applied contrastive pre-training and node clustering to overcome this issue. Leveraging the capabilities of LLMs, Zhu et al. (2023) designs prompts for various knowledge graph construction tasks. Another line of research has aimed to extract knowledge from LLMs to construct KGs (Bosselut et al., 2019; Hao et al., 2023; West et al., 2022). Additionally, PiVe (Han et al., 2023a) utilizes iterative verification prompts to rectify errors in KGs generated by larger LLMs.

3 Methodology

Figure 1 illustrates the proposed framework, referred to as Enhanced LLM with Knowledge Pre-learning and Feedback (ELPF).

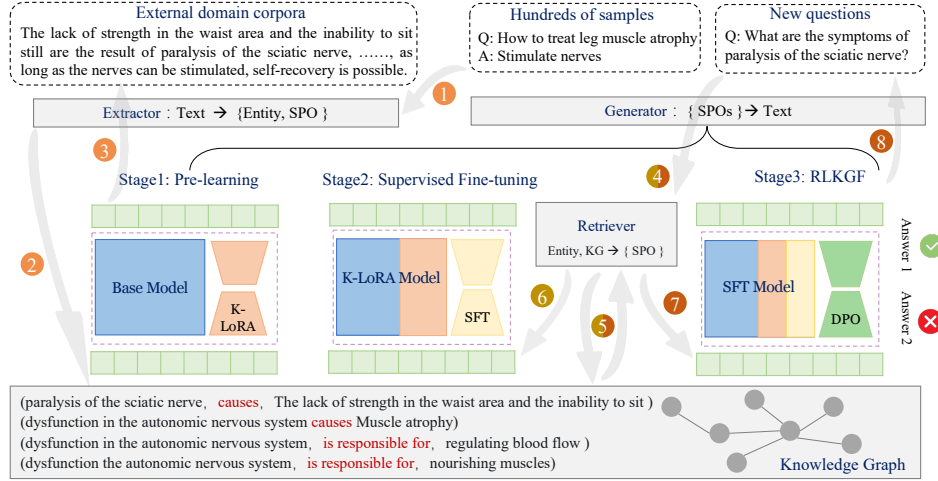


Figure 1: The ELPF framework can be divided into four main stages. 1) **Efficient construction of domain KGs** The process entails labeling a limited set of examples and developing a LLM-based knowledge extraction system to construct a domain KG from corpora efficiently. 2) **Pre-learning with K-LoRA**: Gain an understanding of domain-specific knowledge through LoRA-based triples-to-text generation, referred as K-LoRA. 3) **SFT with KG retrieval**: It involves retrieving subgraphs from the domain-specific KG, modifying the input accordingly and performing supervised fine-tuning. 4) **RLKGF**: The KG acts as an evaluator, providing feedback on knowledge correctness and enabling the model to better align with domain knowledge.

3.1 Efficient construction of domain KGs

For tasks within a specific domain, public available knowledge graphs fail to meet our needs frequently, referred as knowledge mismatch. To counter this issue, a viable solution is to establish a domain-specific knowledge graph utilizing extensive corpora. For one unsupervised document $d \in \mathcal{D}$, the process of KG construction can be formalized as Formula 1.

$$\{\mathcal{S}^a, \mathcal{P}, \mathcal{O}^a\} = \mathcal{F}(d) \quad (1)$$

where \mathcal{F} is KG construction system, \mathcal{S}^a is set of subjects, \mathcal{P} is set of defined relationships and \mathcal{O}^a is set of objects.

The knowledge triples in the results are organized in the form of Formula 2.

$$\mathcal{T}_d = [\langle s_1, p_1, o_{11} \rangle, \dots, \langle s_j, p_k, o_{jk} \rangle] \quad (2)$$

where $o_{jk} = o_{jk1}|o_{jk2}| \dots |o_{jkl}$. These triples are assembled and merged based on the same subject-relation pair. For example, "Rome" and "Florence" are both cities of Italy, so the instance should be represented as "*Italy, City, Rome|Florence*".

However, traditional methods of constructing such graphs can be intricate and often depend on substantial manual labor. Here we have designed an efficient KG construction workflow that requires only minimal annotation, leveraging the advanced semantic comprehension capabilities of LLM. We

have streamlined the procedure into three stages: "knowledge triples extraction", "error removal", and "entity resolution".

Initially, we examine prevalent standards or seek guidance from domain experts to define a schema, and then we manually annotate a small set of examples (≈ 100) to generate training data in the format of "text->knowledge triples". Subsequently, we fine-tune a LLM using LoRA, which is a popular parameter-efficient fine-tuning method. Upon merging the trained LoRA parameters into the base model, we perform inference on extensive corpora to derive knowledge triples. Finally, we employ simple post-processing strategies to minimize errors within the extracted triples:

1. Remove results with incorrect output format, such as triples lacking a subject.
2. Remove results where either the subject or object does not appear in the original text.
3. Remove results where the relationship is not in the defined schema.
4. Remove results where the subject and object are the same.

In the entity resolution phase, we utilize an open-source text embedding tool¹ and set a similarity threshold. If the cosine similarity of two subject nodes surpass this threshold, we regard them as equivalent and subsequently combine their respec-

¹<https://github.com/shibing624/text2vec>

234 tive subgraphs. This merging process contributes
235 to the construction of a comprehensive domain-
236 specific knowledge graph.

237 We perform a quality assessment on 200 sam-
238 ples of the extracted results from our experimental
239 datasets, where the precision (the ratio of correct
240 triples to the total number of generated triples) sur-
241 passes 85%. This suggests that the level of noise
242 within the knowledge graph is within an accept-
243 able range. For additional details and statistical
244 outcomes, please refer to Appendix A.

245 3.2 Pre-learning with K-LoRA

246 Given that the triple form of KGs deviates from
247 the natural language, LLMs exhibit limited profi-
248 ciency in processing it. Moreover, acquiring copi-
249 ous amounts of annotated data in specialized do-
250 mains frequently poses a challenge. Consequently,
251 even with fine-tuning, it remains challenging to
252 enhance the model’s capability to leverage infor-
253 mation from KGs. We hypothesize that it might be
254 feasible to devise a method for low-cost, extensive
255 data construction that enables the model to assim-
256 ilate the task format in advance. Fortunately, by
257 inverting the extraction process described earlier,
258 we can create a "triples-to-text" generation task.
259 With extensive fine-tuning on a multitude of in-
260 stances, the model can be trained to recognize the
261 information format infused by the KG. Addition-
262 ally, as the target text is domain-specific, the model
263 is able to acquire the unique linguistic style asso-
264 ciated with that domain. To boost the fine-tuning
265 process’s efficiency, we continue to utilize LoRA-
266 based SFT. We refer to the LoRA obtained in this
267 step as K-LoRA.

268 3.3 SFT with KG retrieval

269 Pre-learning enables LLMs to better comprehend
270 inputs in the triple form. However, it does not
271 directly resolve specific tasks. Consequently, fur-
272 ther refinement through fine-tuning with supervised
273 learning examples remains essential. We adhere to
274 the normal procedure of KG-retrieval-augmented
275 methods (Lewis et al., 2020; Pan et al., 2024),
276 which involves retrieving pertinent subgraphs from
277 the previously established domain-specific KG and
278 modifying the input accordingly. The comprehen-
279 sive input construction is designed to adhere to the
280 following template:

[KG]: $\{g_q\}$

[Instruction]: Refer to the KG and answer the
following question: $\{q\}$

281 An initial observation reveals that the subjects
282 and relations inherent in the subgraphs exhibit a
283 significant correlation with the core purpose of the
284 input query. To leverage this observation, we em-
285 ploy an open-source embedding tool² to encode
286 all (s, p) pairs within the knowledge graph. Subse-
287 quently, we apply the same embedding tool to en-
288 code the input query. This approach facilitates the
289 calculation of similarity scores between the query’s
290 embedding and those of the top-k (s, p) pairs. Fi-
291 nally, we retrieve the corresponding objects from
292 the original knowledge graph for each (s, p) pair
293 and reconstruct them into triples. These triples are
294 subsequently integrated with the input to provide
295 subgraph information. To maximize the benefits
296 provided by K-LoRA, it is crucial to ensure that the
297 representation of the subgraph remains consistent
298 with the format used during the pre-learning phase.
299

300 3.4 RLKGF

301 After SFT, the model may still exhibit hallucina-
302 tions in its responses due to issues such as overfit-
303 ting. Inspired by the RLHF (Reinforcement Learn-
304 ing with Human Feedback) approach (Ziegler et al.,
305 2020; Ouyang et al., 2022), we hope that the knowl-
306 edge graph can serve as an automated evaluator,
307 providing feedback on knowledge correctness of
308 the current response, thereby guiding the model
309 towards further optimization.

310 First, we generate a variety of responses for
311 each query by employing diverse input formats
312 or random seeds. Subsequently, we incorporate the
313 knowledge graph to score and rank these responses.
314 The scoring process entails the utilization of the ex-
315 traction system described in Section 3.1 to extract
316 triples from these responses, which are then com-
317 pared with the knowledge graph to ascertain their
318 correctness. The reward is determined by the num-
319 ber of correctly matched knowledge triples. The
320 formula for calculating the reward is represented
321 by Formula 3.

$$322 \text{reward} = \log(r_{spo} + \alpha * r_e) \quad (3)$$

323 where α is a hyperparameter, r_{spo} represents the
324 number of SPO matches, and r_e represents the
325 number of entity matches. For more details on

²<https://github.com/shibing624/text2vec>

the specific implementation process, please refer to Algorithm 1, where $Jcard$ represents the Jaccard similarity coefficient (Levandowsky and Winter, 1971). Appendix B demonstrates our automatic reward scoring mechanism using a case example.

To facilitate the training process, we utilize the Direct Preference Optimization (DPO) (Rafailov et al., 2023) training strategy, which mitigates sensitivity to reward values, thereby yielding more stable training process. For a comprehensive introduction to the DPO, please refer to Appendix C. This strategy involves creating pairs of samples according to their reward values. It is crucial to discard any pairs where the difference in rewards is not significant (i.e., $reward_{pos} - reward_{neg} \geq thresh$) and handle issues like repetitive generation in positive samples. To assess the extent of duplication within the positive samples, we can determine the ratio of unique clauses to the overall count of clauses following the deduplication process. Should this ratio fall below a predefined threshold, it would indicate the presence of considerable duplication within the sample, which will be dropped then. By utilizing the knowledge graph for automated evaluation, this method eliminates the requirement of manual scoring, thereby reducing labor costs. Another advantage of this approach is that it is not limited by the quantity of supervised samples, which allows for better learning of knowledge correctness.

4 Experimental Settings and Results

4.1 Datasets

We select two biomedical question-answering datasets, CMedQA (Cui and Han, 2020) and BioASQ (Nentidis et al., 2022), for evaluating our model because both demand extensive domain-specific knowledge. CMedQA is a comprehensive dataset of Chinese medical questions and answers, consisting of over 10,000 pairs. In contrast, BioASQ is an English biomedical dataset that includes 4,719 question and answer pairs and 57,360 reference passages. To simulate a scenario with limited samples, we randomly choose 500 instances from each dataset for training and designate 1,000 instances from each for testing. For CMedQA, we employ the answer texts from the non-selected QA pairs as corpora to construct a knowledge graph in a weakly supervised manner. Similarly, with BioASQ, we use all the provided reference passages as the domain-specific corpora.

Algorithm 1 Constructing pairwise samples

Input: Unsupervised questions Q , graph with entities \mathcal{N}^g and SPOs $\{S^g, \mathcal{P}, O^g\}$

- 1: **for** $q \leftarrow Q$ **do**
- 2: $answers = \mathcal{F}(q)$
- 3: **for** $answer \leftarrow answers$ **do**
- 4: $\{S^a, \mathcal{P}, O^a\} = \mathcal{F}_{ie}(answer)$
- 5: $r_{spo} \leftarrow 0, r_e \leftarrow 0$
- 6: **for** $\{s^g, p, o^g\} \leftarrow \{S^g, \mathcal{P}, O^g\}$ **do**
- 7: **if** $Jcard(\{n_s^a, p, n_o^a\}, \{s^g, p, o^g\}) \geq thresh_{sim}$ **then**
- 8: $r_{spo} \leftarrow r_{spo} + 1$
- 9: **end if**
- 10: **end for**
- 11: **for** $n^g \leftarrow \mathcal{N}^g$ **do**
- 12: **if** $n^a = n^g$ **then**
- 13: $r_e \leftarrow r_e + 1$
- 14: **end if**
- 15: **end for**
- 16: $reward = \log(r_{spo} + \alpha * r_e)$
- 17: **end for**
- 18: **for** $ans_{pos}, ans_{neg} \leftarrow answers \times answers$ **do**
- 19: **if** $reward_{pos} - reward_{neg} < thresh$ **then**
- 20: Drop the pairwise sample
- 21: **end if**
- 22: **if** ans_{pos} contains a lot of repetitive content **then**
- 23: Drop the pairwise sample
- 24: **end if**
- 25: **end for**
- 26: **end for**

Output: pairwise samples $[Ans_{pos}, Ans_{neg}]$

4.2 Evaluation Metric

In our evaluation, we employ multiple metrics, including BLEU (n=4), ROUGE-1, ROUGE-2, and ROUGE-L, to assess the performance of the models. In addition to these automated metrics, we also perform manual evaluations based on five dimensions: fluency, relevance to the question, correctness of the core viewpoint, diversity & completeness, and knowledge hallucination, using reference answers as a benchmark. Since it is challenging to assign an absolute score through manual evaluation, we rank the outputs of models under different settings according to various dimensions. A smaller ranking score indicates better performance, e.g. "1" means the best performance.

4.3 Experimental Settings

During the pre-learning stage, we perform fine-tuning of K-LoRA on both base models. The learning rate and number of epochs in the pre-learning stage are $5e-5$ and 3. During the supervised fine-tuning stage, we establish the similarity threshold for subgraph retrieval to 0.9, and select the top-5 subgraphs. For more hyper-parameters and details, please refer to Appendix D.

Model	CMedQA				BioASQ			
	Rouge-1	Rouge-2	Rouge-L	BLEU	Rouge-1	Rouge-2	Rouge-L	BLEU
ChatGPT-3.5	18.77	2.80	14.20	1.78	27.18	9.94	21.14	5.93
LLM-base	19.73	3.22	14.62	1.17	13.46	2.77	8.38	1.20
LLM-base-SFT(No-retrieval)	17.90	2.80	14.41	2.43	27.67	11.57	23.09	7.05
LLM-CP-SFT(No-retrieval)	18.31	2.84	14.71	2.56	26.99	11.31	23.55	7.23
LLM-base-SFT(RAG)	17.94	2.88	14.28	2.98	27.19	11.44	22.78	9.07
GAP	13.23	1.488	10.23	1.82	26.5	11.31	24.37	6.25
ELPF(ours)	19.83	3.86	15.44	3.46	28.55	12.70	24.21	7.79

Table 1: Performance comparison on CMedQA & BioASQ. "CP" indicates "continual pre-trained". We consider continual pre-training as a basic method of domain knowledge infusion, on par with other retrieval-based methods. Consequently, we do not report on the outcomes of hybrid approaches.

Model	CMedQA				BioASQ			
	Rouge-1	Rouge-2	Rouge-L	BLEU	Rouge-1	Rouge-2	Rouge-L	BLEU
ELPF(ours)	19.83	3.86	15.44	3.46	28.55	12.70	24.21	7.79
w/o K-LoRA&RL	18.55	3.19	14.02	2.86	28.17	11.94	23.47	7.11
w/o K-LoRA	18.62	3.33	15.05	2.90	28.21	11.91	23.41	7.24
w/o RL	19.77	3.85	15.31	3.35	28.61	12.31	23.79	7.44
w/o KG retrieval	19.55	3.59	15.28	3.28	28.29	11.91	23.60	7.27

Table 2: Ablation experiment comparison on CMedQA & BioASQ.

4.4 Baselines

Base LLMs: On the CMedQA dataset, we choose ChatGLM2-6B (Zeng et al., 2023) as base model. On the BioASQ dataset, we choose Llama2-chat-7B (Touvron et al., 2023) as base model. Both of the models are initialized with Hugging Face’s pre-trained checkpoints³⁴. Additionally, we opt to utilize the API of ChatGPT-3.5. For the base LLMs, we present the results of querying the model in a zero-shot scenario. Moreover, to compare the difference with basic continual pre-training method, we conduct continual pre-training on the base LLMs using the aforementioned constructed unsupervised corpus. For the settings of hyper-parameters of continual pre-training, please refer to the Appendix D.

No-retrieval Models: We evaluate the performance of base LLMs and continual pre-trained LLMs after LoRA-based SFT with the constructed training set, where the inputs do not contain any retrieval results.

Retrieval-based Models: For KG-level retrieval, we utilize the state-of-the-art KG-to-text method called GAP (Colas et al., 2022) as a baseline. GAP enhances KG-to-text generation by incorporating graph-aware elements into pre-trained language models. For document-level retrieval, we compare our approach with the representative method called

RAG (Lewis et al., 2020). RAG ensures that the text retrieval source aligns with the unsupervised corpus used for KG construction. The retrieval method employed here is the same as the subgraph retrieval approach discussed in Section 3.3. We place the retrieval results on the inputs and then perform LoRA-based SFT.

4.5 Main Results

Our results on the CMedQA and BioASQ datasets are shown in Table 1. We observe that the zero-shot querying method achieved ROUGE scores that are close to those obtained through supervised fine-tuning. However, it is worth noting that the zero-shot querying method results in significantly lower BLEU scores on both datasets. These results indicate that the zero-shot querying method does not effectively balance the professionalism and fluency of the generated text. Consequently, this method may not be suitable for generating domain-specific text that meets the desired criteria.

In terms of fine-tuning-based methods, our model shows improvements across various metrics. On the CMedQA dataset, our model achieves a 1.03 ROUGE-L improvement and a 1.03 BLEU improvement compared to the vanilla LoRA-based SFT method. On the BioASQ dataset, we have achieved a 1.12 improvement in ROUGE-L and a 0.74 improvement in BLEU. It is worth noting that our method achieves a significant performance improvement even compared to continual pre-training

³<https://huggingface.co/THUDM/chatglm2-6b>

⁴<https://huggingface.co/meta-llama/Llama-2-7b-chat-hf>

458 followed by fine-tuning. These results highlight
 459 the effectiveness of our proposed KG collabora-
 460 tive method in enhancing the performance of fine-
 461 tuning for LLM. Compared to the GAP method,
 462 our approach not only exhibits significant improve-
 463 ments but also offers the advantage of not requiring
 464 the full-parameter joint training of a graph encoder
 465 with a pre-trained model like GAP. In compari-
 466 son to RAG, which focuses on document retrieval,
 467 our method achieves higher ROUGE scores but
 468 lower BLEU scores on the BioASQ dataset. This
 469 difference may be attributed to the document re-
 470 trieval system’s ability to recall more extensive
 471 information. On the other hand, the process of con-
 472 structing a KG introduces information loss, which
 473 results in ELPF generation relying more on the im-
 474 plicit knowledge of LLM itself when the subgraph
 475 is insufficient, leading to lower accuracy. At the
 476 same time, document retrieval also introduces more
 477 noise, leading to some answers deviating from the
 478 original question.

479 5 Analysis

480 5.1 Ablation Studies

481 We conduct several ablation experiments to evalu-
 482 ate the effectiveness of each module. These experi-
 483 ments involve the individual removal of K-LoRA,
 484 KG prompt, and RLKGF, as well as the simulta-
 485 neous removal of both K-LoRA and RLKGF. The
 486 results of these experiments, including ROUGE
 487 and BLEU scores, can be found in Table 2. Addi-
 488 tionally, the manual evaluation results for BioASQ
 489 are presented in Figure 2. Here are the key obser-
 490 vations from our analysis: (1) Removing K-LoRA
 491 leads to the most significant performance drop, re-
 492 flected in ROUGE, BLEU, and the diversity of
 493 knowledge. The main reason is that the format
 494 of triples-to-text training samples is similar to the
 495 format of the subsequent fine-tuning task, allow-
 496 ing the model to better incorporate the knowledge
 497 implied by the input. (2) RLKGF has a less signifi-
 498 cant impact on ROUGE and BLEU metrics. This
 499 is because the reinforcement objective is not fo-
 500 cused on replicating the target answer, but rather
 501 on incorporating comprehensive, effective, and ac-
 502 curate domain knowledge. It improves the diver-
 503 sity of knowledge, as well as the correctness of
 504 viewpoints, and reduces hallucinations, achieving
 505 the goal of reinforcement learning. (3) The re-
 506 sults of manual evaluation indicate that the ablated
 507 models with knowledge integration demonstrate

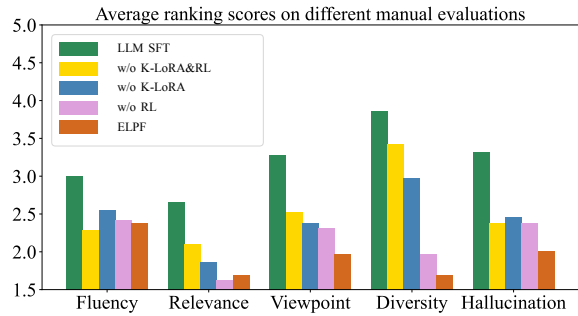


Figure 2: On the BioASQ dataset, different methods are ranked based on five human evaluation dimensions: fluency, relevance to the question, correctness of the core viewpoint, diversity & completeness, and knowledge hallucination. The ranking score represents the manual ranking of the content generated by different models, where a lower ranking score indicates higher quality of the generated content.

508 improvements over the baseline model that relies
 509 solely on fine-tuning, in terms of knowledge cor-
 510 rectness (question relevance, viewpoint correctness,
 511 and hallucinations) and knowledge diversity. Our
 512 ELPF method outperforms others across all dimen-
 513 sions, demonstrating its effectiveness. Appendix E
 514 presents a specific case, which allows for a more
 515 intuitive understanding of the effectiveness of the
 516 answers output by different models.

517 5.2 In-depth Analysis of K-LoRA

518 To further analyze the overall impact of K-LoRA
 519 on the model, we will examine its effects on do-
 520 main awareness and the alignment of generated
 521 text with the knowledge graph. K-LoRA aims

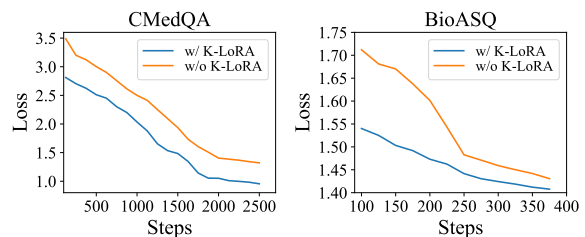


Figure 3: The loss curve of ELPF was compared under the same settings, with and without K-LoRA.

521 to enable the LLM to pre-learn within the current
 522 domain and generate text with the assistance of
 523 the knowledge graph in a weakly supervised man-
 524 ner. Regarding domain awareness, as illustrated
 525 in Fig.3, we observe a reduction in loss during
 526 the model training process and find that the model
 527 fused with K-LoRA not only has a smaller initial
 528 loss but also converges faster. This indicates that
 529

Question
What could be the cause of menstrual period back pain that lasts for a long time?
Reference
Introduction to dysmenorrhea: Dysmenorrhea refers to the occurrence of lower abdominal pain, lower back pain, lower abdominal bloating, or other discomfort before, during, or after the menstrual period, which can significantly affect daily life and work. According to traditional Chinese medicine, this is often caused by blood stasis. Taking some traditional Chinese medicines that promote blood circulation and remove blood stasis can be used for treatment. Options include Nujin Pill and Motherwort Cream.
Retrieved subgraph
<Dysmenorrhea, clinical manifestations, lower abdominal pain low back pain lower abdominal bloating other discomforts > <Dysmenorrhea, etiology, blood stasis > <Dysmenorrhea, medication treatment, Nujin Pill Motherwort Cream >
ELPF
Menstrual period back pain is caused by blood stasis , which can be alleviated by taking Chinese patent medicine Xiaoyao Pill and Nujin Pill for regulation. Additionally, taking Motherwort Cream in combination can help relieve the symptoms of dysmenorrhea.
ELPF w/o K-LoRA
It is considered to be menstrual irregularities. There are many reasons that can cause menstrual irregularities, such as endocrine disorders, gynecological inflammation, and psychological/environmental factors. It is recommended that you actively go to the hospital for a blood HCG test to determine if it is gynecological inflammation. Treatment should be administered accordingly.

Figure 4: Case study on impact on information compliance of K-LoRA. Information provided by KG in text is highlighted.

the model develops a certain level of awareness of the current domain through the training and weight fusion of K-LoRA. Therefore, K-LoRA serves as a straightforward and efficient approach for domain learning. In terms of the information compliance of the generated text to the knowledge graph, we analyze the text generated with and without K-LoRA, as shown in Figure 4. We notice that although the same knowledge graph information is provided, the original model does not effectively utilize this knowledge graph for generation. On the other hand, the model integrated with K-LoRA relies more on the knowledge graph and generates answers that are closer to the reference answers. This is because the task format of pre-learning and SFT is similar, and K-LoRA enhances the model’s ability to adapt to input from the knowledge graph.

5.3 Knowledge Completeness

As our approach depends on information from the knowledge graph, this section explores the impact of the knowledge graph’s completeness on our method. The completeness of knowledge can be measured by the size and quality of the knowledge graph. First, we explore the influence of graph size. We offer various sizes of KG, including full

(100%), 80%, 60%, 40%, 20%, and 0%. The size control is achieved by randomly removing a certain proportion of nodes from the entire graph. Next, we investigate the impact of graph quality. We construct a set of target data to simulate the upper limit of model performance. The target data consists of triples extracted from the reference answers that correspond to the questions. The results are shown in Table 3. Firstly, we find that reducing the size of the knowledge graph does lead to a decrease in performance, but it is not a purely positive relationship. This is because our knowledge graph contains noise, and the model needs to balance between useful information and noise during the learning process. The model cannot effectively learn when the graph is sparse, resulting in even worse performance compared to not incorporating the graph information. Secondly, we observe that the current results still exhibit a certain gap when compared to the results obtained from the target data. This indicates that there is room for improvement in the quality of the graph constructed by LLM and the subgraph retrieval method. We will address these issues in future work.

	CMedQA		BioASQ	
	Rouge-L	BLEU	Rouge-L	BLEU
0 %	15.04	2.97	23.70	7.23
20%	14.98	3.02	23.59	7.14
40%	15.12	2.95	24.20	7.61
60%	15.26	3.10	24.39	7.70
80%	15.30	3.22	24.39	7.68
100%	15.44	3.46	24.21	7.79
target	16.40	3.56	25.32	8.03

Table 3: The performance comparison on knowledge completeness.

6 Conclusions

In this work, we propose a framework for efficiently infuse domain knowledge into LLMs. By employing efficient construction of domain knowledge graphs and a three-stage KG-LLM alignment process, we address the issues of knowledge mismatch and poor information compliance. Experiments demonstrate that our method significantly improves the quality of text generation and knowledge correctness in limited sample scenarios. We hope our work will provide insight into the challenge of connecting KG with LLM in future exploration.

592 Limitations

593 Although ELPF is relatively friendly in terms
594 of sample size and computational resources, this
595 method still has certain limitations. Since the con-
596 struction of the domain knowledge graph is re-
597 quired in both SFT and RLKGF, the ELPF method
598 is highly dependent on the quality of the graph
599 construction. However, our graph is established
600 based on weak supervision signals, so there are
601 inevitably noises in the results. Insufficient noise
602 handling can affect the effectiveness of the method.
603 Furthermore, because the self-built domain knowl-
604 edge graph (KG) is incomplete, it is challenging to
605 detect knowledge errors unless they conflict with
606 known knowledge. Additionally, determining the
607 relevance of the knowledge to the query is a vague
608 concept that is difficult to assess. Therefore, to en-
609 hance the stability and versatility of reinforcement
610 learning, we have adopted a more conservative rein-
611 forcement strategy in RLKGF. This approach some-
612 what limits the optimization space. However, in
613 actual vertical domain application scenarios, the
614 positive reinforcement or conflict penalty strategies
615 can be adjusted according to the actual situation
616 to achieve better results. Finally, our method fo-
617 cuses on domain-specific text generation. However,
618 due to the limited availability of appropriate public
619 datasets, we only conducted experiments on medi-
620 cal domain texts. This limitation may pose a risk
621 to the generalized ability of our findings in other
622 scenarios.

623 References

624 Zhijie Bao, Wei Chen, Shengze Xiao, Kuang Ren, Jiao
625 Wu, Cheng Zhong, Jiajie Peng, Xuanjing Huang, and
626 Zhongyu Wei. 2023. [Disc-medllm: Bridging gen-
627 eral large language models and real-world medical
628 consultation.](#)

629 Sebastian Borgeaud, Arthur Mensch, Jordan Hoff-
630 mann, Trevor Cai, Eliza Rutherford, Katie Milli-
631 can, George Bm Van Den Driessche, Jean-Baptiste
632 Lespiau, Bogdan Damoc, Aidan Clark, et al. 2022.
633 Improving language models by retrieving from tril-
634 lions of tokens. In *International conference on ma-
635 chine learning*, pages 2206–2240. PMLR.

636 Antoine Bosselut, Hannah Rashkin, Maarten Sap, Chai-
637 tanya Malaviya, Asli Celikyilmaz, and Yejin Choi.
638 2019. [COMET: commonsense transformers for auto-
639 matic knowledge graph construction.](#) In *Proceedings
640 of the 57th Conference of the Association for Compu-
641 tational Linguistics, ACL 2019, Florence, Italy, July
642 28- August 2, 2019, Volume 1: Long Papers*, pages

4762–4779. Association for Computational Linguistics. 643
644

Anthony Colas, Mehrdad Alvandipour, and Daisy Zhe
Wang. 2022. [GAP: A graph-aware language model
framework for knowledge graph-to-text generation.](#)
In *Proceedings of the 29th International Conference
on Computational Linguistics*, pages 5755–5769,
Gyeongju, Republic of Korea. International Com-
mittee on Computational Linguistics. 645
646
647
648
649
650
651

Xiongtao Cui and Jungang Han. 2020. [Chinese
medical question answer matching based on inter-
active sentence representation learning.](#) volume
abs/2011.13573. 652
653
654
655

Jiuzhou Han, Nigel Collier, Wray Buntine, and Ehsan
Shareghi. 2023a. [Pive: Prompting with iterative veri-
fication improving graph-based generative capability
of llms.](#) 656
657
658
659

Tianyu Han, Lisa C. Adams, Jens-Michalis Papaioan-
nou, Paul Grundmann, Tom Oberhauser, Alexander
Löser, Daniel Truhn, and Keno K. Bressem. 2023b.
[Medalpaca – an open-source collection of medical
conversational ai models and training data.](#) 660
661
662
663
664

Shibo Hao, Bowen Tan, Kaiwen Tang, Bin Ni, Xiyan
Shao, Hengzhe Zhang, Eric P. Xing, and Zhiting Hu.
2023. [Bertnet: Harvesting knowledge graphs with
arbitrary relations from pretrained language models.](#)
In *Findings of the Association for Computational
Linguistics: ACL 2023, Toronto, Canada, July 9-14,
2023*, pages 5000–5015. Association for Computa-
tional Linguistics. 665
666
667
668
669
670
671
672

Chenxu Hu, Jie Fu, Chenzhuang Du, Simian Luo, Junbo
Zhao, and Hang Zhao. 2023. [Chatdb: Augmenting
llms with databases as their symbolic memory.](#) 673
674
675

Edward J. Hu, Yelong Shen, Phillip Wallis, Zeyuan
Allen-Zhu, Yuanzhi Li, Shean Wang, Lu Wang, and
Weizhu Chen. 2021. [Lora: Low-rank adaptation of
large language models.](#) 676
677
678
679

Gautier Izacard and Edouard Grave. 2021. [Leveraging
passage retrieval with generative models for open do-
main question answering.](#) In *Proceedings of the 16th
Conference of the European Chapter of the Associ-
ation for Computational Linguistics: Main Volume,
EACL 2021, Online, April 19 - 23, 2021*, pages 874–
880. Association for Computational Linguistics. 680
681
682
683
684
685
686

Pei Ke, Haozhe Ji, Yu Ran, Xin Cui, Liwei Wang, Lin-
feng Song, Xiaoyan Zhu, and Minlie Huang. 2021.
[JointGT: Graph-text joint representation learning for
text generation from knowledge graphs.](#) In *Find-
ings of the Association for Computational Linguis-
tics: ACL-IJCNLP 2021*, pages 2526–2538, Online.
Association for Computational Linguistics. 687
688
689
690
691
692
693

Tian Lan, Deng Cai, Yan Wang, Heyan Huang, and
Xian-Ling Mao. 2023. [Copy is all you need.](#) In
*The Eleventh International Conference on Learning
Representations.* 694
695
696
697

698	Michael Levandowsky and David K. Winter. 1971. Distance between sets . <i>Nature</i> , 234:34–35.	
699		
700	Patrick Lewis, Ethan Perez, Aleksandra Piktus, Fabio	
701	Petroni, Vladimir Karpukhin, Naman Goyal, Hein-	
702	rich Küttler, Mike Lewis, Wen-tau Yih, Tim Rock-	
703	täschel, et al. 2020. Retrieval-augmented generation	
704	for knowledge-intensive nlp tasks. volume 33, pages	
705	9459–9474.	
706	Junyi Li, Tianyi Tang, Wayne Xin Zhao, Zhicheng Wei,	
707	Nicholas Jing Yuan, and Ji-Rong Wen. 2021. Few-	
708	shot knowledge graph-to-text generation with pre-	
709	trained language models . In <i>Findings of the Associa-</i>	
710	<i>tion for Computational Linguistics: ACL-IJCNLP</i>	
711	<i>2021</i> , pages 1558–1568, Online. Association for	
712	Computational Linguistics.	
713	Ling Luo, Po-Ting Lai, Chih-Hsuan Wei, Cecilia N	
714	Arighi, and Zhiyong Lu. 2022. BioRED: a rich	
715	biomedical relation extraction dataset . volume 23,	
716	page bbac282.	
717	Sewon Min, Weijia Shi, Mike Lewis, Xilun Chen, Wen-	
718	tau Yih, Hannaneh Hajishirzi, and Luke Zettlemoyer.	
719	2023. Nonparametric masked language modeling .	
720	In <i>Findings of the Association for Computational</i>	
721	<i>Linguistics: ACL 2023, Toronto, Canada, July 9-14,</i>	
722	<i>2023</i> , pages 2097–2118. Association for Computa-	
723	tional Linguistics.	
724	Fedor Moiseev, Zhe Dong, Enrique Alfonseca, and Mar-	
725	tin Jaggi. 2022. SKILL: Structured knowledge infu-	
726	sion for large language models . In <i>Proceedings of</i>	
727	<i>the 2022 Conference of the North American Chap-</i>	
728	<i>ter of the Association for Computational Linguistics:</i>	
729	<i>Human Language Technologies</i> , pages 1581–1588,	
730	Seattle, United States. Association for Computational	
731	Linguistics.	
732	Anastasios Nentidis, Georgios Katsimpras, Eirini	
733	Vandorou, Anastasia Krithara, Antonio Miranda-	
734	Escalada, Luis Gasco, Martin Krallinger, and Geor-	
735	gios Paliouras. 2022. Overview of BioASQ 2022:	
736	The tenth BioASQ challenge on large-scale biomed-	
737	ical semantic indexing and question answering . In	
738	<i>Lecture Notes in Computer Science</i> , pages 337–361.	
739	Springer International Publishing.	
740	OpenAI. 2022. Chatgpt: Optimizing language models	
741	for dialogue.	
742	Long Ouyang, Jeff Wu, Xu Jiang, Diogo Almeida, Car-	
743	roll L. Wainwright, Pamela Mishkin, Chong Zhang,	
744	Sandhini Agarwal, Katarina Slama, Alex Ray, John	
745	Schulman, Jacob Hilton, Fraser Kelton, Luke Miller,	
746	Maddie Simens, Amanda Askell, Peter Welinder,	
747	Paul Christiano, Jan Leike, and Ryan Lowe. 2022.	
748	Training language models to follow instructions with	
749	human feedback .	
750	Shirui Pan, Linhao Luo, Yufei Wang, Chen Chen, Ji-	
751	apu Wang, and Xindong Wu. 2024. Unifying large	
752	language models and knowledge graphs: A roadmap .	
753	<i>IEEE Transactions on Knowledge and Data Engi-</i>	
754	<i>neering</i> , pages 1–20.	
	Hongjing Qian, Yutao Zhu, Zhicheng Dou, Haoqi Gu,	755
	Xinyu Zhang, Zheng Liu, Ruofei Lai, Zhao Cao,	756
	Jian-Yun Nie, and Ji-Rong Wen. 2023. Webbrain:	757
	Learning to generate factually correct articles for	758
	queries by grounding on large web corpus .	759
	Rafael Rafailov, Archit Sharma, Eric Mitchell, Stefano	760
	Ermon, Christopher D Manning, and Chelsea Finn.	761
	2023. Direct preference optimization: Your language	762
	model is secretly a reward model .	763
	Priyanka Ranade and Anupam Joshi. 2023. Fabula:	764
	Intelligence report generation using retrieval-	765
	augmented narrative construction . <i>ArXiv</i> ,	766
	abs/2310.13848.	767
	Hugo Touvron, Louis Martin, Kevin Stone, Peter Al-	768
	bert, Amjad Almahairi, Yasmine Babaei, Nikolay	769
	Bashlykov, Soumya Batra, Prajjwal Bhargava, Shruti	770
	Bhosale, Dan Bikel, Lukas Blecher, Cristian Canton	771
	Ferrer, Moya Chen, Guillem Cucurull, David Esiobu,	772
	Jude Fernandes, Jeremy Fu, Wenyin Fu, Brian Fuller,	773
	Cynthia Gao, Vedanuj Goswami, Naman Goyal, An-	774
	thony Hartshorn, Saghar Hosseini, Rui Hou, Hakan	775
	Inan, Marcin Kardas, Viktor Kerkez, Madian Khabsa,	776
	Isabel Kloumann, Artem Korenev, Punit Singh Koura,	777
	Marie-Anne Lachaux, Thibaut Lavril, Jenya Lee, Di-	778
	ana Liskovich, Yinghai Lu, Yuning Mao, Xavier Mar-	779
	tinet, Todor Mihaylov, Pushkar Mishra, Igor Moly-	780
	bog, Yixin Nie, Andrew Poulton, Jeremy Reizen-	781
	stein, Rashi Rungta, Kalyan Saladi, Alan Schelten,	782
	Ruan Silva, Eric Michael Smith, Ranjan Subrama-	783
	nian, Xiaoqing Ellen Tan, Binh Tang, Ross Tay-	784
	lor, Adina Williams, Jian Xiang Kuan, Puxin Xu,	785
	Zheng Yan, Iliyan Zarov, Yuchen Zhang, Angela Fan,	786
	Melanie Kambadur, Sharan Narang, Aurelien Ro-	787
	driguez, Robert Stojnic, Sergey Edunov, and Thomas	788
	Scialom. 2023. Llama 2: Open foundation and fine-	789
	tuned chat models .	790
	Xintao Wang, Qianwen Yang, Yongting Qiu, Jiaqing	791
	Liang, Qianyu He, Zhouhong Gu, Yanghua Xiao,	792
	and Wei Wang. 2023. Knowledgept: Enhancing large	793
	language models with retrieval and storage access on	794
	knowledge bases .	795
	Peter West, Chandra Bhagavatula, Jack Hessel, Jena D.	796
	Hwang, Liwei Jiang, Ronan Le Bras, Ximing Lu,	797
	Sean Welleck, and Yejin Choi. 2022. Symbolic	798
	knowledge distillation: from general language mod-	799
	els to commonsense models . In <i>Proceedings of the</i>	800
	<i>2022 Conference of the North American Chapter of</i>	801
	<i>the Association for Computational Linguistics: Hu-</i>	802
	<i>man Language Technologies, NAACL 2022, Seattle,</i>	803
	<i>WA, United States, July 10-15, 2022</i> , pages 4602–	804
	4625. Association for Computational Linguistics.	805
	Siwei Wu, Xiangqing Shen, and Rui Xia. 2023. Com-	806
	monsense knowledge graph completion via con-	807
	trastive pretraining and node clustering . In <i>Find-</i>	808
	<i>ings of the Association for Computational Linguis-</i>	809
	<i>tics: ACL 2023, Toronto, Canada, July 9-14, 2023</i> ,	810
	pages 13977–13989. Association for Computational	811
	Linguistics.	812

813 Shicheng Xu, Liang Pang, Huawei Shen, Xueqi Cheng,
814 and Tat-seng Chua. 2023. Search-in-the-chain: To-
815 wards the accurate, credible and traceable content
816 generation for complex knowledge-intensive tasks.

817 Seunghak Yu, Tianxing He, and James Glass. 2021.
818 [Autokg: Constructing virtual knowledge graphs from](#)
819 [unstructured documents for question answering.](#)

820 Aohan Zeng, Xiao Liu, Zhengxiao Du, Zihan Wang,
821 Hanyu Lai, Ming Ding, Zhuoyi Yang, Yifan Xu,
822 Wendi Zheng, Xiao Xia, Weng Lam Tam, Zixuan Ma,
823 Yufei Xue, Jidong Zhai, Wenguang Chen, Zhiyuan
824 Liu, Peng Zhang, Yuxiao Dong, and Jie Tang. 2023.
825 [GLM-130B: an open bilingual pre-trained model.](#)

826 Xinlu Zhang, Chenxin Tian, Xianjun Yang, Lichang
827 Chen, Zekun Li, and Linda Ruth Petzold. 2023.
828 [Alpacare:instruction-tuned large language models for](#)
829 [medical application.](#)

830 Yuqi Zhu, Xiaohan Wang, Jing Chen, Shuofei Qiao,
831 Yixin Ou, Yunzhi Yao, Shumin Deng, Huajun Chen,
832 and Ningyu Zhang. 2023. Lms for knowledge graph
833 construction and reasoning: Recent capabilities and
834 future opportunities.

835 Daniel M. Ziegler, Nisan Stiennon, Jeffrey Wu, Tom B.
836 Brown, Alec Radford, Dario Amodei, Paul Chris-
837 tiano, and Geoffrey Irving. 2020. [Fine-tuning lan-
838 guage models from human preferences.](#)

839 A Weakly Supervised Domain-specific IE 840 System Construction

841 For the annotation standard of the CMedQA
842 dataset, we referred to the CMeIE v2 dataset⁵,
843 which is a large-scale Chinese medical domain rela-
844 tion extraction dataset. For BioASQ, we referred to
845 BioRED (Luo et al., 2022), an English medical re-
846 lation extraction dataset annotated on the PubMed
847 data source.

848 The types of relationship defined in the
849 CMedQA dataset are: ["Differential Diagnosis",
850 "Pathological Typing", "Clinical Manifestation",
851 "Adjuvant Therapy", "Pharmacotherapy", "Surgi-
852 cal Treatment", "Etiology", "Synonyms", "Imaging
853 Examination", "Auxiliary Examination", "Depart-
854 ment of Consultation", "Complications", "Labora-
855 tory Test", "Susceptible Population", "Genetic Fac-
856 tors", "High-risk Factors", "Pathogenesis", "Site
857 of Onset", "Medical History", "Incidence Rate",
858 "Prognosis", "Age of Onset", "Prevention", "Post-
859 treatment Symptoms", "Pathophysiology", "Trans-
860 mission Route", "Peak Season", "Histological
861 Examination", "Stage", "Radiotherapy", "Screen-
862 ing", "Chemotherapy", "Risk Assessment Factors",

⁵<https://tianchi.aliyun.com/dataset/95414>

"Metastatic Sites", "Prevalence Area", "Mortality
863 Rate"]. 864

865 The types of relationship defined in the
866 BioASQ dataset are: ["Association", "isa", "Nega-
867 tive_Correlation", "Positive_Correlation"].

868 For each reference dataset, we only utilized its
869 relational schema and manually annotated 100 sam-
870 ples sampled from unsupervised corpora.

871 During manual annotation, we assigned two an-
872 notators for blind labeling and one quality control
873 personnel for inspection. The final inter-annotator
874 agreement was 0.9, and the accuracy of acceptance
875 was 0.97. During the training, we employed the
876 generative information extraction paradigm and
877 trained a LoRA on top of LLM. The hyperparame-
878 ter settings were consistent with those in the SFT
879 stage.

880 Statistical details of the constructed graph are
881 provided in Table 4. The symbol "#" denotes a
882 sign for counting. We performed a quality assess-
883 ment on 200 samples of the extracted results from
884 experimental datasets and calculated the precision
885 (the ratio of correct triples to the total number of
886 generated triples).

Datasets	#Subjects	#Triples	Precision
CMedQA	25963	220111	0.85
BioASQ	20922	53209	0.89

886 Table 4: Statistics of the constructed domain KGs.

887 B Automated Reward Function

888 In RLKGF, we primarily propose an automated
889 reward scoring mechanism that integrates a Knowl-
890 edge Graph (KG). Here, we will demonstrate this
891 process through a specific case study as show in
892 Fig.5. For detailed information about the reward
893 calculation, please refer to Algorithm 1.

894 C Direct Preference Optimiz ation (DPO)

895 Construct a static pairwise dataset $\mathcal{D} =$
896 $\{x^i, y_\omega^i, y_l^i\}_{i=1}^N$ according to Section 3.3, where y_ω
897 represents the positive samples and y_l represents
898 the negative samples, and then perform reward
899 modeling. According to DPO, the reward model
900 $r_\phi(x, y)$ is trained using a negative log-likelihood
901 loss as follows:

$$902 \mathcal{L} = -\mathbb{E}_{(x, y_\omega, y_l) \sim \mathcal{D}} [\log \theta(r_\phi(x, y_\omega) - r_\phi(x, y_l))] 902$$

903 where θ is the logistic function. In the context
904 of LMs, the network $r_\phi(x, y)$ is often initialized

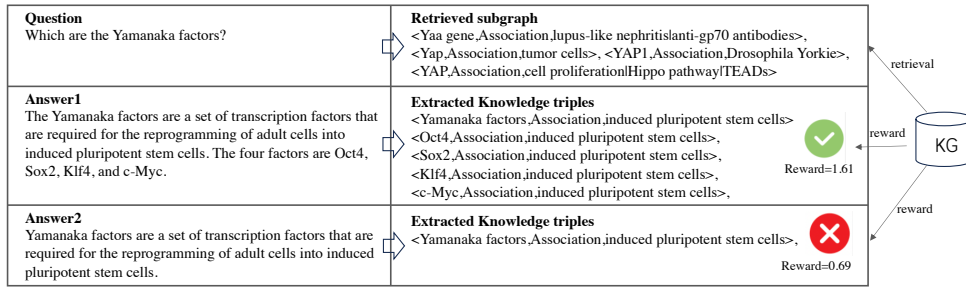


Figure 5: Case study on RLKGF dataset generation.

	CMedQA			BioASQ		
	K-LoRA	SFT	RLKGF	K-LoRA	SFT	RLKGF
LLM	ChatGLM2-6B			Llama2-chat-7B		
batch size	32	32	8	32	32	8
fine-tuning type	LoRA	LoRA	LoRA	LoRA	LoRA	LoRA
epochs	3	20	1	3	3	1
lora rank	8	8	8	8	8	8
lora target	QKV	QKV	QKV	QKVO	QKVO	QKVO
learning rate	$5e^{-5}$	$1e^{-4}$	$1e^{-6}$	$5e^{-5}$	$5e^{-5}$	$1e^{-6}$
max-input-length	512	512	512	512	512	512
max-output-length	512	512	512	512	512	512
KL-div β	-	-	0.4	-	-	0.4
top-p	0.7	0.7	0.7	0.7	0.7	0.7
temperature	0.9	0.9	0.9	0.01	0.01	0.01

Table 5: The parameter settings on CMedQA and BioASQ.

Q	Which are the main causes of fetal echogenic bowel?			
Reference	<p>Fetal echogenic bowel is mainly associated to feto-maternal, intramniotic bleeding but in several cases it is linked to cystic fibrosis, cytomegalovirus (CMV), herpes simplex virus and other viral infections and fetal aneuploidy.</p> <p>KG information: [<fetal aneuploidy,Association,Cytomegalovirus>’, <fetal aneuploidy,Association,herpes simplex virus>’, <fetal aneuploidy,Association,cystic fibrosis>’, <fetal aneuploidy,Association,feto-maternal>’, <fetal echogenic bowel,Association,fetal aneuploidy>’]</p>			
Comparisons	<p>ChatGPT 3.5 Fetal echogenic bowel refers to a condition where there is increased brightness or echogenicity of the fetal bowel on ultrasound. It can be associated with several possible causes, including:</p> <ol style="list-style-type: none"> 1. Maternal Factors: Certain maternal conditions can contribute to fetal echogenic bowel. These may include infections such as cytomegalovirus (CMV), toxoplasmosis, or parvovirus B19. Maternal diabetes and intrauterine growth restriction (IUGR) can also be associated with this condition. 2. Genetic Disorders: Fetal echogenic bowel can be a marker for certain genetic disorders. It is commonly seen in cases of trisomy 21 (Down syndrome), but can also be associated with other chromosomal abnormalities such as trisomy 18 (Edwards syndrome) or trisomy 13 (Patau syndrome). 3. Fetal Infections: In some cases, fetal infections can cause echogenic bowel. These may include intrauterine infections such as CMV, toxoplasmosis, or rubella. 4. Bowel Obstruction or Meconium Peritonitis: Certain conditions that affect the fetal bowel, such as bowel obstruction or meconium peritonitis (inflammation of the lining of the abdominal cavity due to the leakage of meconium), can lead to echogenic bowel. <p>It is important to note that the presence of fetal echogenic bowel does not always indicate a serious problem, as it can be a benign finding in some cases. However, it should be evaluated further by a healthcare professional to determine the underlying cause and any associated risks or implications for the baby.</p>	<p>LLAMA2 SFT Fetal echogenic bowel (FEB) is a common sonographic finding in the second trimester of pregnancy. The main causes of fetal echogenic bowel are:</p> <ol style="list-style-type: none"> 1. Intrahepatic cholestasis of pregnancy (ICP) 2. Fetal bile duct obstruction 3. Fetal bile acid synthesis 4. Fetal bile acid transport 5. Fetal bile acid metabolism 		
Outs	<p>ELPF Fetal echogenic bowel (FEB) is a sonographic finding characterized by the presence of echogenic bowel loops in the fetal abdomen. It is a common finding in the first trimester of pregnancy and is usually benign. However, it may be associated with several fetal anomalies, such as cystic fibrosis, herpes simplex virus, and structural malformations.</p>	<p>ELPF w/o K-LoRA&RL Fetal echogenic bowel (ECHO) is a common sonographic finding in the second trimester of pregnancy. It is characterized by the presence of a hyperechoic bowel wall, which is thought to be due to the accumulation of bile and/or meconium in the bowel lumen.</p>	<p>ELPF w/o K-LoRA Fetal echogenic bowel is a common sonographic finding in the second trimester of pregnancy. It is associated with intrauterine fetal demise, IUGR, aneuploidy, structural malformations, growth deficiency, and pregnancy complications.</p>	<p>ELPF w/o RL Fetal echogenic bowel (FEB) is a sonographic finding characterized by the presence of a hyperechoic bowel wall. It is a common sonographic finding in the second trimester of pregnancy and is usually benign. However, it may be associated with several fetal anomalies, such as cystic fibrosis, aneuploidy, and structural malformations.</p>

Figure 6: Performance of various models in one case.

905 from the SFT model $\pi^{SFT}(y|x)$ with the addition
 906 of a linear layer on top of the final transformer
 907 layer that produces a single scalar prediction for
 908 the reward value. To ensure a reward function with
 909 lower variance, prior works normalize the rewards,
 910 such that $\mathbb{E}_{(x,y)\sim\mathcal{D}}[r_\phi(x,y)] = 0$ for all x . During
 911 the DPO RL phase, use the learned reward function
 912 to provide feedback to the language model, with
 913 the optimization objective as follows:

$$\mathcal{J} = \max_{\pi_\theta} \mathbb{E}_{x\sim\mathcal{D}, y\sim\pi_\theta(y|x)} [r_\phi(x,y)] - \beta \mathbb{D}_{KL}[\pi_\theta(y|x) || \pi_{ref}(y|x)]$$

914
 915 where β is a parameter that controls deviation from
 916 the baseline reference policy π_{ref} , and constraints
 917 on the KL divergence ensure that the reinforced
 918 strategy does not deviate too far from the base-
 919 line reference strategy (SFT). We also analyzed
 920 the impact of the value of the β parameter on the
 921 reinforcement training and selected an optimal pa-
 922 rameter for subsequent training, as seen in Table 6.

	Rouge-1	Rouge-2	Rouge-L	BLEU
$\beta=0.1$	28.1	11.81	23.29	7.2
$\beta=0.2$	28.2	11.88	23.36	7.25
$\beta=0.4$	28.61	12.27	23.81	7.42

Table 6: In BioASQ, performance comparison of ELPF on different parameters β .

923 D Implementation Details

924
 925 We conduct experiments on four A100 80GB GPUs
 926 and two V100 32GB GPUs. For details of the pa-
 927 rameters used in the experimental training at each
 928 stage, please refer to Table 5. As for continual pre-
 929 training, we fine-tune full parameter of LLM with
 930 batch_size=4, epochs=3, learning_rate=5e-5.

931 E Case Study

932 We evaluate the effectiveness of the model through
 933 several case studies, as shown in Figure 6. ELPF
 934 provided concise and relatively comprehensive an-
 935 swers regarding the characteristics and main causes
 936 of fetal intestinal echoes. It mentioned both phys-
 937 iological and pathological situations. ELPF(w/o
 938 RLKGF) is close to ELPF in performance. How-
 939 ever, the other answers were not as complete.
 940 ELPF(w/o K-LoRA&RLKGF) only mentions the
 941 physiological condition, while ELPF(w/o K-LoRA)
 942 only addresses the pathological factors. Untrained

models like ChatGPT-3.5 and Llama2-chat-7B ex-
 hibit obvious hallucinations.

943
 944